The role of cGMP and the rear of the cell in Dictyostelium chemotaxis and cell streaming

Veltman, Douwe M.; van Haastert, Peter J. M.

Published in:
Journal of Cell Science

DOI:
10.1242/jcs.015602

Publication date:
2008

The role of cGMP and the rear of the cell in *Dictyostelium* chemotaxis and cell streaming

Douwe M. Veltman and Peter J. M. van Haastert*

Department of Biology, University of Groningen, Kerklaan 30, 9751 NN Haren, The Netherlands

*Author for correspondence (e-mail: P.J.M.van.haastert@rug.nl)

Accepted 22 October 2007
J. Cell Sci. 121, 120-127 Published by The Company of Biologists 2008
doi:10.1242/jcs.015602

Summary

During chemotaxis, pseudopod extensions lead the cell towards the source of attractant. The role of actin-filled pseudopodia at the front of the cell is well recognized, whereas the function of the rear of the cell in chemotaxis and cell-cell interactions is less well known. *Dictyostelium* cell aggregation is mediated by outwardly propagating waves of extracellular cAMP that induce chemotaxis and cell-cell contacts, resulting in streams of cells moving towards the aggregation centre. Wild-type cells efficiently retract pseudopodia in the rear of the cell during the rising flank of the cAMP wave and have a quiescent cell posterior. This polarization largely remains during the declining flank, which causes cells to continue their chemotactic movement towards the aggregation centre and to form stable streams of moving cells. The dominance of the leading-edge pseudopod rescues chemotaxis during the rising flank of the wave, but the cells move in random directions after the peak of the wave has passed. As a consequence, cell-cell contacts cannot be maintained, and the cell streams break up. The results show that a quiescent rear of the cell increases the efficiency of directional movement and is essential to maintain stable cell-cell contacts.

Supplementary material available online at
http://jcs.biologists.org/cgi/content/full/121/1/120/DC1

Key words: Guanylyl cyclase, Polarity, *Dictyostelium*, Chemotaxis, Streaming

Introduction

The development of a group of single amoeboid *Dictyostelium* cells into a multicellular fruiting body is accomplished by coordinated chemotaxis in accord with the wave patterns of extracellular cAMP. The developmental program initiates when a few starved cells start to secrete cAMP. Neighbouring cells move towards the cAMP source and relay the signfig. 1al. This leads to the formation of a concentric cAMP wave pattern around the initial source, which becomes the centre of aggregation (Alcantara and Monk, 1974). Typically, ~15-20 cAMP waves traverse through the population, during which cells become elongated and polarized (Swanson and Taylor, 1982) and then connect to each other in a head-to-tail fashion. This results in the formation of cell streams that extend all the way to the borders of the aggregation territory and guide the cells efficiently to the centre of aggregation.

The signals at the leading edge during cell migration are relatively well understood (Merlot and Firtel, 2003; Van Haastert and Devreotes, 2004). However, the rear of the cell must be important as well because chemotaxis will be impaired when the rear of the cell is not effectively retracted. Conventional myosin (henceforth referred to as myosin) is a heterohexamer of two myosin heavy chains, two myosin regulatory light chains and two myosin essential light chains. Myosin is an important component of the cytoskeleton in the rear of the cell and its function is regulated by a number of different signal transduction pathways (Bosgraaf and van Haastert, 2006; de la Roche et al., 2002). The incorporation of myosin in the cytoskeleton in *Dictyostelium* in response to a cAMP stimulus is dependent on cGMP, which is generated from GTP by guanylyl cyclase (Bosgraaf et al., 2002). The *Dictyostelium* genome encodes two guanylyl cyclases, a membrane-bound guanylyl cyclase (GCA) and a soluble guanylyl cyclase (sGC) (Roelofs et al., 2001a; Roelofs et al., 2001b). The primary target of cGMP is the cGMP-binding protein C (GbpC). Activation of GbpC results in an increase in phosphorylation of the myosin regulatory light chain and a transient uptake of myosin filaments in the cell cortex (Bosgraaf et al., 2002). During cell migration, myosin filaments are found mostly in the cortex of the rear of the cell, where they are involved in retraction of the uropod (Clow and McNally, 1999). Cells lacking the cGMP response have an aberrant cell posterior. Levels of myosin in the rear of the cell are reduced and the cells show an increased number of lateral pseudopodia (Bosgraaf et al., 2002; Veltman and Van Haastert, 2006).

Here, we used mutant cells that are disrupted with respect to cGMP signalling to investigate the function of the rear of the cell during development of *Dictyostelium* cells. We find that a quiescent rear of the cell is essential for the maintenance of directional movement in between subsequent cAMP waves. In addition, a quiescent rear is important for stable cell-cell interactions during streaming. The combined defects of reduced chemotaxis and unstable cell-cell contacts of mutants with defective cGMP signalling lead to poor cell aggregation and the formation of only small fruiting bodies.

Results

Impaired cell streaming and development of cGMP mutants in monolayers

We examined the development of both wild-type AX3 and *gc*-null cells, applied as a monolayer on non-nutrient agar. Both genes encoding guanylyl cyclases are disrupted in *gc*-null cells, and thus

these cells are unable to synthesize cGMP. The typical spiral wave formation started 4 hours after the onset of starvation in both AX3 and in *gc*-null cells, which indicates that the cAMP relay is not impaired in the *gc*-null mutant. Approximately 5 hours after the onset of starvation, the monolayer breaks up. The average size of an aggregation territory of *gc*-null cells is ~12 mm^2. This is somewhat smaller than the territory size of wild-type cells, which is ~22 mm^2. However, the most pronounced difference in development between wild-type cells and *gc*-null cells becomes apparent when streams are formed. Wild-type cells form continuous streams towards the aggregation centre, whereas streams of *gc*-null cells are highly fragmented (Fig. 1). The panel with the higher magnification shows that the edges of streams of wild-type cells are smooth. Cells in these streams are elongated and do not extend lateral pseudopodia outside of the stream. By contrast, streams of *gc*-null cells are very irregular. Cells in these streams are relatively nonpolar and frequently extend pseudopodia outside of the stream. The fragmentation of *gc*-null cell streams results in the formation of many small aggregates. Further development of these small aggregates is relatively normal as they proceed through the slug phase and culminate in the formation of fruiting bodies with the same timing as that of wild-type cells. Owing to the smaller aggregate size, the nascent fruiting bodies are substantially smaller. The streaming defect of *gc*-null cells could not be rescued by starving the cells for a prolonged time in shaken suspension before plating them out, indicating that the streaming defect is not the result of an aberrant developmental timing event (data not shown). The streaming defect of *gc*-null cells was observed in confluent cell monolayers of approximately 1×10^6 cells/cm^2 in Fig. 1 and at a lower cell density of 2.5×10^5 cells/cm^2 in Fig. 2 but also at even lower cell densities of 5×10^4 cells/cm^2 (data not shown).

To ensure that the observed streaming defect of the *gc*-null cell strain originates from the disruption of the genes encoding guanylyl cyclase, the *sgc* gene was expressed in *gc*-null cells in order to effect a rescue. During cell aggregation, sGC mediates more than 90% of the cAMP-induced cGMP production and GCA less than 10% (Roelofs and Van Haastert, 2002). Rescued cells showed smooth uninterrupted streams and formed fruiting bodies that are comparable in size to wild-type fruiting bodies. The streaming phenotype of *gc*-null cells must therefore originate from the lack of the sGC enzyme and cGMP synthesis. To investigate further the observed streaming defect, several properties of *gc*-null cells were examined that are important for cell streaming, such as chemotaxis and the ability to establish cell contacts.

Chemotaxis efficiency during aggregation

The chemotaxis of individual cells during early aggregation was investigated by recording time-lapse movies at a relatively high magnification (see supplementary material Movies 1-4). During early aggregation, cAMP spiral waves direct the cells to the centre of aggregation. At the start of the movie, cells from both strains are individual and are dispersed homogeneously (Fig. 2A, t=0 minutes). All cells periodically and simultaneously make short surges towards the aggregation centre in response to the natural cAMP waves that are travelling through the field. By the end of the movie, cells from the wild-type strain are all oriented towards the aggregation centre and incorporated into smooth streams, whereas cells from the *gc*-null strain are still fairly nonpolar and clumped irregularly together (Fig. 2A, t=60 minutes).

The trajectories of >25 cells in each movie were tracked and their chemotaxis parameters were quantified. Only individual cells were taken into account, and tracking of a cell was stopped as soon as it entered a stream. Tracks of three representative cells are shown in Fig. 2B. The average speed and chemotaxis index (the ratio of the displacement of a cell in the direction of the gradient versus its total distance travelled) of cells from both strains show periodic changes throughout aggregation (Fig. 2C). Wild-type cells show relatively small surges in cell speed during the first waves. Later waves induce increasingly greater responses, but, in between the

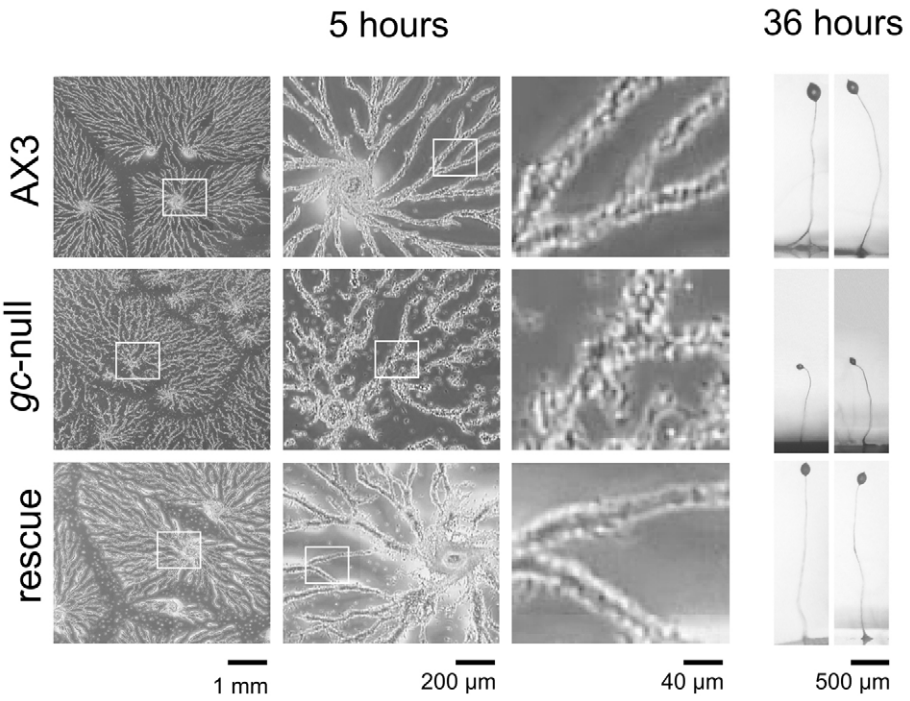

Fig. 1. Development of *gc*-null cells. Wild-type AX3, *gc*-null and rescued *gc*-null cells were settled as a monolayer on non-nutrient agar plates and allowed to starve (t=0). Pictures of developing cells were taken during aggregation (t=5 hours) and after completion of formation of fruiting bodies (t=36 hours). To illustrate better the differential behaviour of the cell strains during aggregation, the area in the white box of the first panel is enlarged in the second panel and further enlarged in the third panel. Black bars indicate the scales used for each picture.

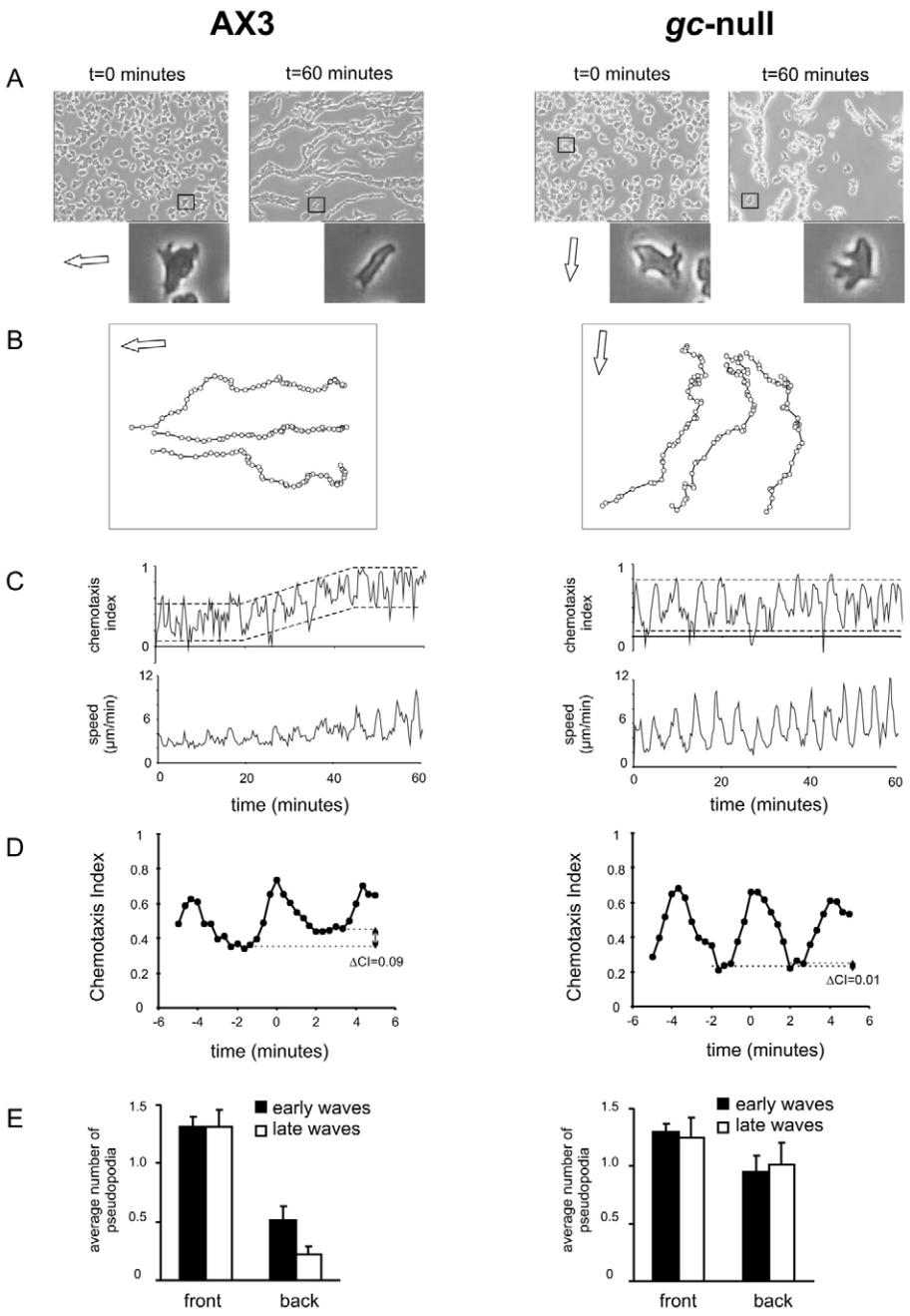

Fig. 2. Speed and chemotaxis index during aggregation. (A) Wild-type AX3 and *gc*-null cells were allowed to aggregate on non-nutrient agar plates, and a movie of the aggregating cells was recorded (supplementary material Movies 1 and 2). The chemotaxis of the cells was analyzed from the time-point where cells first make a simultaneous movement surge in the direction of the aggregation centre (t=0 minutes) until the time-point where most cells are incorporated into streams (t=60 minutes). A representative cell in each frame is enlarged in the bottom frame. The arrow points in the direction of the aggregation centre, which is out of view. (B) The position of 25 cells was tracked throughout the duration of the movie. Cell tracks of three representative cells are shown. The tracks start at t=0 and are followed for at least 40 minutes. Unfilled dots were placed on the cell tracks representing the positions at intervals of 1 minute. Cells move in the direction of the aggregation centre, as indicated by the arrow. (C) The average chemotaxis index and speed of the cells was determined in each movie. The dotted lines indicate the progress of the minimum and maximum chemotaxis index, respectively, during the course of aggregation. The period where the minimum chemotaxis index increases with each subsequent wave is referred to as the 'transition period'. (D) The waves of the chemotaxis index of aggregating cells during the transition period of two independent movies were averaged. Time on the horizontal scale is relative to the time-point of the peak of the wave. The ΔCI that is indicated in the graph is the difference between the average of the lowest three points of the chemotaxis index both before and after the wave. (E) The number of protrusions in the front one-third and rear one-third of the cell was determined throughout aggregation. The graph shows the average number of pseudopodia during the first four waves and the last four waves of the movie. Error bars indicate the standard deviation.

peaks, the speed keeps returning to approximately the same basal level of 3 μm/minute. In addition to the effect on cell speed, early waves also induce a small increase in the chemotaxis index. In between the peaks of the first 5-7 waves, the chemotaxis index drops back to almost zero. Thus, the acquired orientation in response to a cAMP wave is entirely lost before the next wave arrives at the cells. However, the minimum chemotaxis index in between the next 5-6 waves increases from 0 to ~0.5. This period, where the minimum chemotaxis index increases with each subsequent wave, will be referred to as the transition period. After this transition period, the minimum chemotaxis index in between waves remains fairly constant at 0.5 until the cells are incorporated into streams.

The main difference between wild-type and *gc*-null cells is that, in *gc*-null cells, every subsequent wave induces essentially identical responses and that the transition period is absent. The cell speed in aggregating *gc*-null cells shows large surges at a relatively early stage, and, somewhat surprisingly, the chemotaxis index also shows large increases in response to early cAMP waves. However, in contrast to wild-type cells, the acquired orientation is lost in between all subsequent waves. This complete loss of chemotaxis index in between waves persists until the end of the movie, where most cells are incorporated into irregular streams and individual cells can no longer be tracked.

An important difference of chemotaxis in natural waves between wild-type and *gc*-null cells is the ability of wild-type cells to retain orientation at the back of the wave during and after the transition period. To investigate further this difference between wild-type and *gc*-null cells, the responses from two independent movies were averaged over the 5-6 waves of the transition period in order to

reduce the variation. For *gc*-null cells, we used the same number of waves from the period that corresponds to the transition period of wild-type cells. In these averaged waves, it can be seen that the chemotaxis index during the rising flank of the natural cAMP wave increases similarly in wild-type and *gc*-null cells (Fig. 2D). Cells from both strains show an increase of chemotaxis index of 0.4 in a period of ~1 minute. By contrast, the recovery of the chemotaxis index at the back of the wave shows a noticeable difference between cells from both strains. The chemotaxis index of *gc*-null cells rapidly declines after reaching the peak value and, when the next wave arrives in *gc*-null cells, the chemotaxis index has recovered completely. The chemotaxis index of wild-type cells decreases at a much slower rate than that of *gc*-null cells. When the next wave arrives in wild-type cells, the chemotaxis index of the previous wave has not yet recovered. This results in an increase of chemotaxis index of ~0.09 with each subsequent wave in this phase. As the transition period comprises 5-6 waves, wild-type cells have obtained a minimum chemotaxis index of ~0.5 in the troughs of the cAMP waves after the transition period.

gc-null cells have a hyperactive rear of the cell

Cells lacking guanylyl cyclase are known to have an increased number of lateral pseudopodia during chemotaxis, whereas wild-type cells usually have a very smooth posterior. We counted the number of protrusions in the front one-third and rear one-third of the cell throughout aggregation in each movie. The data were grouped for the first four waves of the movie, where all cells are still individual and for the last 4 waves in the movie, at the onset of stream formation (Fig. 2E). In the front one-third of the cell, the number of protrusions was remarkably stable. Both wild-type and *gc*-null cells have an average of ~1.3 protrusions in the front one-third of the cells, and this number changes only a little throughout aggregation ($P>0.5$ for wild-type and $P<0.5$ for *gc*-null cells). However, the numbers of protrusions in the back of the cell show some marked differences. Wild-type cells have rather few (0.53±0.12) protrusions in the rear one-third of the cell. This number decreases to 0.28±0.09 as aggregation progresses, which is significantly less than the number of lateral pseudopodia during the first waves ($P<0.05$). By contrast, *gc*-null cells have more protrusions (0.78±0.23) in the rear one-third of the cell during the first natural cAMP waves. More importantly, *gc*-null cells do not seem to be able to regulate the number of lateral pseudopodia, as the number stays the same throughout aggregation. At the onset of streaming, the number of observed lateral pseudopodia is still 0.88±0.24, which is not significantly different compared with that recorded during the first waves of the movie ($P>0.5$).

Recent work has shown that new pseudopodia of wild-type cells are formed primarily by the splitting of existing pseudopodia (Andrew and Insall, 2007). Of the two split pseudopodia, one is retracted, mostly rapidly in the front of the cell, but sometimes much later in the rear of the cell. We examined whether the increased number of protrusions that are observed in the rear of *gc*-null cells were actually made in the back of the cell or originate from the improper retraction of pseudopodia that were made in the front. The frequent occurrence of cell-cell contacts during natural aggregation prevents the tracking of pseudopodia over a prolonged time, which complicates tracking the origin of pseudopodia. Therefore, movies were recorded at lower cell densities, and cells were exposed to a shallow static gradient using a modified Zigmond chemotaxis chamber (see supplementary material Movies 3 and 4). In still images under these conditions, 17.5% of all pseudopodia are observed in the back one-third of wild-type cells, and 46.0% of all pseudopodia are observed in the back one-third of *gc*-null cells (Table 1). The results show that, in wild-type cells, only ~4% of the pseudopodia are actually made in the posterior one-third of the cell. Thus, nearly all pseudopodia that are visible at any given time in the cell posterior of wild-type cells originate from the front of the cell. By contrast, in *gc*-null cells, as many as 23.2% of all pseudopodia were protruded from the posterior one-third of the cell, and this accounts for half of the pseudopodia that are visible in the posterior of *gc*-null cells at any given time, with the other half of the posterior pseudopodia originating from the front of the cell. We conclude that *gc*-null cells extend approximately sixfold more pseudopodia in the rear of the cell than extended by wild-type cells.

Table 1. Initiation of lateral pseudopodia

	Percentage of pseudopodia that are observed at the cell rear at any given time	Percentage of pseudopodia that are produced at the cell rear
Wild type	17.5±4.9	3.97±2.63
gc-null	46.0±1.7	23.20±4.50
gc-null + sGCΔN	19.2±2.7	3.85±2.71
gc-null + sGCΔcat	35.7±3.1	21.43±2.87

Cells from the indicated strains were subjected to a shallow spatial cAMP gradient and allowed to move by chemotaxis. Four independent cells were tracked, and, for each visible pseudopod, it was determined at what position along the perimeter of the cell it was initiated. The average number of pseudopodia (± s.d.) visible in the posterior one-third of the cell at any time is shown in the left column. The average number of pseudopodia (± s.d.) initiated in the posterior one-third of the cell, with at least 21 pseudopodia per track, is shown in the right column.

Cell-cell contact sites

Streaming *Dictyostelium* cells adhere to each other using the cell-adhesion protein Contact site A (Beug et al., 1973; Muller et al., 1979). The observed stream fragmentation of *gc*-null cells could potentially be augmented by a reduced expression or functional activity of this protein. Cell adhesions that are mediated by Contact site A remain intact when treated with 10 mM EDTA. Therefore, we measured the development of EDTA-resistant cell contacts during starvation of wild-type and *gc*-null cells in shaking culture (Fig. 3A). Early starved cells from both strains make no EDTA-resistant cell contacts. Shortly after initiation of cAMP pulses, which was after 3 hours in this experiment, as indicated by the dashed line in the figure, both wild-type and *gc*-null cells start to make EDTA-resistant cell contacts. After 6 hours, all cells from both strains are incorporated into cell clumps. The observation that development of EDTA-resistant cell contacts of *gc*-null cells is similar to that of wild-type cells indicates that the stream fragmentation of *gc*-null cells is not caused by a reduced expression or functional activity of the Contact site A protein.

Stream initiation and termination

Mutants that do not generate a cAMP signal in the rear of the cell, such as cells null for the gene encoding adenylyl cyclase A, act as stream terminators during aggregation (Kriebel et al., 2003). Other cells do not connect to the rear of adenylyl cyclase A-null cells, and therefore these cells are always found at the last position of a stream when they are allowed to aggregate in mixtures with wild-type cells. We investigated whether *gc*-null cells function as stream terminators by mixing equal amounts of wild-type and *gc*-null cells

and allowing them to aggregate. GFP was expressed in one of the cell strains in order to discriminate between strains. Lower cell densities were used as, under these conditions, a large number of small aggregates are formed with short, thin streams, where individual head-to-tail cell contacts can readily be identified. The average length of the cell trains under these conditions was approximately five cells. At the first position of the stream, an approximately equal percentage of cells from each strain was found, indicating that *gc*-null cells are still good stream initiators (Fig. 3B). Somewhat unexpectedly, relatively few *gc*-null cells were found in the middle (26±9%) and tail (34±9%) positions of the streams. Thus, *gc*-null cells do not act as stream terminators, but are less efficient in following a leading cell. As a consequence, *gc*-null cells are under-represented in the cells streams (35% of all cells in streams are *gc*-null cells). The experiment with AX3–*gc*-null (GFP) mixtures yielded the same result as with AX3(GFP)–*gc*-null mixtures, indicating that the expression of GFP did not have any effect on the relative position of the cell in the stream.

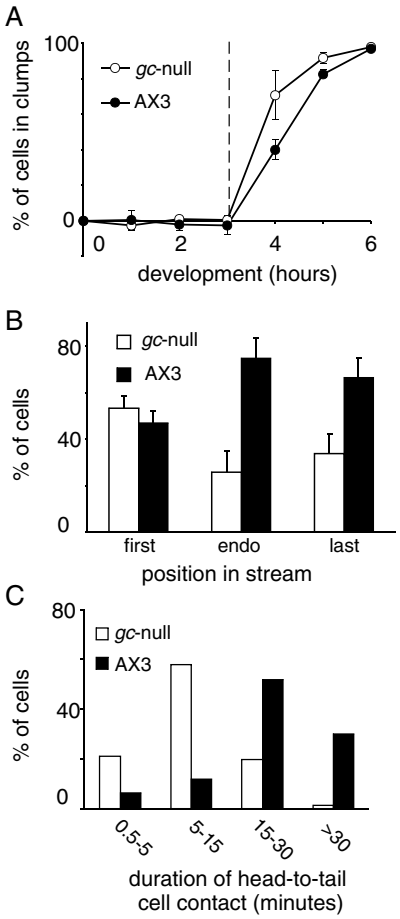

Fig. 3. Properties of cell contacts. (A) Wild-type AX3 and *gc*-null cells were starved in shaking suspension at 1×10^7 cells/ml. Cells were pulsed with 30 nM cAMP, starting at 3 hours after the onset of starvation, indicated by the dashed line in the figure. Each hour, a sample was drawn and incubated for 15 minutes in 10 mM EDTA. The number of cells that made no cell contact with other cells was determined using a haemocytometer. On the basis of these numbers, the percentage of cells in clumps was calculated. Each time-point was taken in duplicate and the experiment was repeated twice. Error bars indicate the standard deviation. (B) Either AX3 or *gc*-null cells were labelled with GFP. An equal amount of unlabeled starved cells from one strain was mixed with starved, labelled cells from the other strain, and the mixed cell suspension was settled on non-nutrient agar at 5×10^4 cells/cm^2. After one hour of aggregation, thin streams of single-cell width were visible. Each cell in such a cell stream making polar head-to-tail contacts was identified as either a wild-type or *gc*-null cell. The graph shows the percentage of cells from each strain at the first position, middle (endo) positions and last position. The assay was repeated four times [two experiments with AX3(GFP)/*gc*-null and two experiments with AX3/*gc*-null (GFP) cells]. Error bars indicate the standard deviation. In total, 164 cell trains were analysed. (C) Starved wild-type and *gc*-null cells were settled on non-nutrient agar at a density of 5×10^4 cells/cm^2 and a movie was recorded. The duration of all head-to-tail cell contacts that lasted for >30 seconds was noted and plotted as a percentage of the total number of cells analysed. The experiment was repeated two times and >90 individual head-to-tail cell contacts were analysed for each strain.

The foregoing results demonstrate that *gc*-null cells have normal cell-cell adhesion and stream initiation. When starved as a confluent monolayer, *gc*-null cells also have a reasonable chemotactic response to natural cAMP waves, which allows them to reach the end of existing streams. This suggests that initiation of head-to-tail cell-cell contacts in streams is mostly intact in *gc*-null cells. Instead, the observed streaming defect of *gc*-null cells might be caused by a higher occurrence of dissociation from streams. As a measure of the stream dissociation rate, the average duration of individual head-to-tail cell contacts of aggregating wild-type and *gc*-null cells was quantified (Fig. 3C). Only head-to-tail cell contacts that lasted for >30 seconds were taken into account in order to exclude coincidental contacts. Most of the wild-type cells maintained head-to-tail cell contacts for 15 to 30 minutes and ~30% of the cells maintained the contact for even longer than 30 minutes. By contrast, most of the *gc*-null cells maintained their polar head-to-tail contact for 5-15 minutes and only 1% maintained contact for >30 minutes. This indicates that the short streams observed in aggregating *gc*-null cells originate mostly from an increase in stream break-up rather than a decreased rate of stream formation.

cGMP pathway

The cGMP pathway consists of several components (Bosgraaf et al., 2002). Most of the cGMP during aggregation is produced by the action of sGC (Roelofs and Van Haastert, 2002). The downstream target of cGMP is the GbpC protein, and activation of this protein results in the redistribution of myosin. We examined the streaming behaviour of sGC and GbpC mutants to confirm whether the observed streaming defect is transduced through this pathway. As the sGC protein has an additional function during chemotaxis that is independent of formation of cGMP, the reduced polarity of *gc*-null cells during aggregation could potentially be caused by the lack of the sGC protein itself instead of the lack of a cGMP response The protein localizes to the leading edge during chemotaxis, which leads to a decrease in the amount of turning (Veltman and Van Haastert, 2006). Cells that are *gc*-null expressing a truncated sGC protein, termed sGCΔN, that no longer localizes to the leading edge but is still catalytically active show uninterrupted smooth streams of wild-type cells (Fig. 4). By contrast *gc*-null cells expressing the catalytically inactive, but anteriorly located sGCΔcat, show the typical stream break-up of *gc*-null cells. The improved orientation of cells expressing catalytically inactive sGCΔcat that was observed in static spatial gradients (Veltman and Van Haastert, 2006) is therefore not responsible for the persistent orientation in between cAMP waves during natural aggregation. Instead, this property appears to be fully dependent on the formation of cGMP.

Knockout cells of the cGMP target protein GbpC show a streaming defect that is similar, but somewhat more severe, to that of *gc*-null cells. Spiral wave formation appears normal, but the cell

monolayer breaks up into many small aggregates at a relatively early stage, even before the separation of the aggregation territories becomes visible. As with *gc*-null cells, the small aggregates develop into relatively normal, but small, fruiting bodies.

Discussion

We have investigated the function of cGMP signalling and its regulation of the rear of the cell during natural aggregation by analysing the behaviour of *Dictyostelium* mutants lacking guanylyl cyclase activity. Cells lacking cGMP signalling extend considerably more pseudopodia in the rear of the cell, resulting in a decreased stability of head-to-tail cell contacts and the break-up of cell streams.

Chemotaxis

Mutant *gc*-null cells are still able to extend a pseudopod in the direction of the gradient but fail to properly retract pseudopodia that are misaligned. These lateral pseudopodia lead to a decreased efficiency of chemotaxis in stable spatial gradients and shallow spatiotemporal gradients (Bosgraaf et al., 2002; Veltman and Van Haastert, 2006). The increased number of lateral pseudopodia is also observed when tracking *gc*-null cells that are migrating up the gradient of natural cAMP waves, but, somewhat surprisingly, these cells attain a chemotaxis index during the rising flank of the wave that is comparable to that of wild-type cells. The peak of the chemotaxis index in *gc*-null cells is accompanied by a large surge in cell speed. Apparently, the pseudopodia in the direction of the gradient are extending faster and further than pseudopodia at the sides and at the back of the cell (Fig. 5A, lower-left panel). The relatively strong spatiotemporal gradient at the rising flank of the wave presumably fully activates signalling pathways that are responsible for pseudopod extension at the leading edge. This dominance of the leading-edge pseudopod results in both an increase in cell speed and a good chemotaxis index, whereas the lateral pseudopodia make no significant contribution to cell displacement.

The difference in efficiency of chemotaxis between wild-type and *gc*-null cells is most pronounced during the declining flank of the cAMP wave. Wild-type cells become 'trained' within approximately ten cAMP waves, after which cells stably suppress pseudopodia in the rear of the cell during the rising flank of the cAMP wave and retain this polarization during the declining flank of the cAMP wave. By contrast, *gc*-null cells never become trained. The polarity that is built up during the rising flank of the cAMP wave is lost after the peak of the cAMP wave has passed (Fig. 5A,

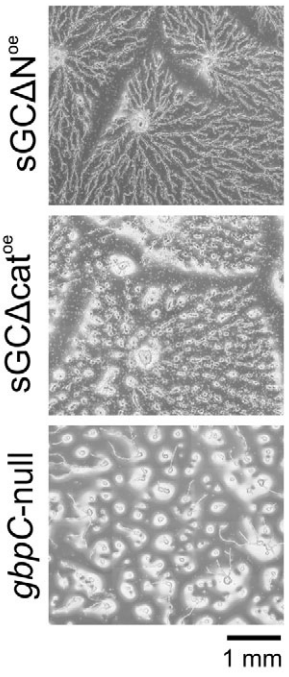

Fig. 4. Development of cGMP-mutant cell strains. Mutant cells were starved as a monolayer on non-nutrient agar plates. Pictures of developing cells were taken at 5 hours after the start of starvation. *gc*-null cells lack cGMP synthesis, whereas *gpbC*-null cells lack the cGMP-target protein GbpC that mediates cell polarity. sGCΔN, expressed in *gc*-null cells, is catalytically active but cytosolic. sGCΔcat is catalytically inactive but localizes to the anterior of the cell, an event that previously was shown to stabilize the leading edge in a spatial gradient.

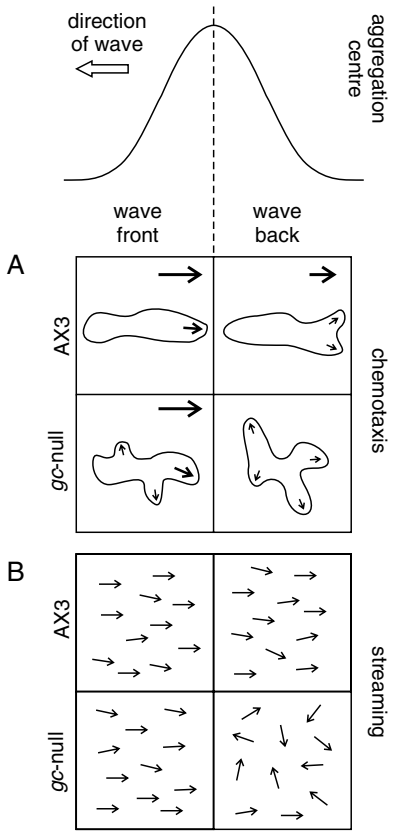

Fig. 5. Proposed model of the effects of a stable rear of the cell on chemotaxis, cell-cell contact and cell streaming. (A) The strong spatiotemporal gradient at the rising flank of a cAMP wave induces a dominant pseudopod in both wild-type and *gc*-null cells. Wild-type cells suppress pseudopod formation in the posterior half of the cell. *gc*-null cells have an increased number of lateral pseudopodia, but their contribution to cell movement is relatively small during this phase. During the second half of the wave, wild-type cells maintain their polarized cell shape and extend pseudopodia only in the front. In the absence of a gradient-induced dominant pseudopod, the increased number of lateral pseudopodia in *gc*-null cells lead to a rapid decrease of directional cell migration during the second half of the cAMP wave. (B) The polarity of wild-type cells that is acquired during the first half of the wave results in a persistent orientation towards the aggregation centre in the second half of the wave. By contrast, *gc*-null cells, which do not properly polarize, lack the orientation towards the aggregation centre during the back of the wave. This decreased orientation leads to movement in apparently random directions and an increased tendency to break out of cell streams.

bottom-right panel). We conclude that *gc*-null cells have a hyperactive rear of the cell. During the rising flank of the cAMP wave, the pseudopodia at the leading edge are dominant and the protrusions in the rear of the cell are ineffective for cell movement. However, after the peak of the cAMP wave has passed, the protrusions in the rear of the cell become as effective as the protrusions in the front of the cell, and *gc*-null cells exhibit random movement. By contrast, wild-type cells have a quiescent rear in the back of the cAMP wave, and the pseudopod in the front of the cell persists as the only determiner of cell movement.

The current observations of wild-type and *gc*-null cells during aggregation are in good agreement with previous results obtained from the *stmF* mutant. This mutant was isolated on the basis of its property of forming long aggregation streams when grown on bacterial plates (Ross and Newell, 1979). *stmF* cells are defective in cGMP phosphodiesterase activity and therefore have an enhanced and prolonged cGMP response (Ross and Newell, 1981; van Haastert et al., 1982). When *stmF* cells are allowed to aggregate as a monolayer on non-nutrient agar, the cells remain unusually elongated in the back of the wave (Chandrasekhar et al., 1995; Ross and Newell, 1981). This behaviour is essentially the opposite of that of cells lacking cGMP signalling. The combined observations provide firm evidence for the role of cGMP signalling in the control of polarity during aggregation and cell streaming.

cGMP regulates the phosphorylation of the myosin regulatory light chain and the incorporation of myosin into the cytoskeleton. Streaming defects have also been described in several myosin heavy chain and light chain mutants, indicating that the aberrant regulation of myosin function in cGMP-mutant cell strains might be the cause of their streaming defects. A mutant in which the phosphorylatable serine of myosin regulatory light chain was replaced by an alanine showed an increased speed and chemotaxis efficiency (Zhang et al., 2002). Cells remained unusually elongated in the back of natural cAMP waves, a morphological phenotype that is also seen in *stmF* cells. However, cell streams of an aggregating monolayer of myosin regulatory light chain mutant cells showed an increased stream fragmentation, in contrast to the observed long streams of *stmF* cells. Incorporation of myosin in the cytoskeleton is regulated by the phosphorylation state of the myosin heavy chain at three threonine residues. A 3xASP myosin-heavy-chain mutant (threonine residues replaced by threonine-phosphate-mimicking aspartate residues) has reduced myosin incorporation into the cytoskeleton; the mutant exhibits very poor chemotaxis, does not stream and forms a large number of aggregates during development (Heid et al., 2004). Cells expressing a 3xALA mutant (threonine residues replaced by non-phosphorylatable alanine residues) have an increased amount of cortical myosin, a moderate chemotaxis index and respond well to natural cAMP waves (Heid et al., 2004). However, monolayers of aggregating mutant cells still show an increased rate of stream break-up. The combined data suggest that only through properly regulated phosphorylation and dephosphorylation of myosin in response to the different phases of a natural wave can the correct morphological responses be generated that are essential for cell streaming and that the trapping of myosin in one specific state by constitutively active or inactive phosphorylation mutants is inhibitory for stream formation.

The present results also provide a new view on the old 'back of the wave' problem for *Dictyostelium* chemotaxis. During the rising flank of the wave, cells rapidly migrate in the direction of the cAMP gradient towards the centre of aggregation. But, as the wave passes by, the cAMP concentration gradient is reversed, potentially directing the cells away from the aggregation centre. The general idea is that cell movement freezes at the top of the cAMP wave and that cells resume moving in random directions during the declining flank and in between the cAMP waves (Soll et al., 2002; Wessels et al., 1989). We can confirm this notion for the first six or so waves of wild-type cells and essentially for all waves of *gc*-null cells. However, during later cAMP waves, wild-type cells do not lose polarity at the declining flank of the wave but retain the direction of movement that they obtained during the rising flank of the wave. Previously, the 'back of the wave' problem has been investigated using well-controlled experiments with simulated temporal waves (Varnum-Finney et al., 1987; Varnum et al., 1985; Wessels et al., 1989; Wessels et al., 2000). It was found that, at the peak of a temporal wave, cells stop extending new pseudopodia, round up and start to move in random directions. A possible explanation for the different observations in simulated temporal waves in comparison with natural waves might be the lack of spatial information in the simulated temporal waves. Spatial gradients, especially those of cAMP waves during late cell aggregation, induce strong internal functional polarization of wild-type cells. This polarity is derived from the suppression of pseudopodia at the sides and at the rear of the cell. The polarity that is built up during the rising flank of the wave might be the driving force behind directional migration during the declining flank of the wave. Cells in simulated temporal waves lack the gradient-induced internal polarization and therefore move in a random fashion after the cAMP concentration peak has passed.

Stream formation

During early starvation, cells start to migrate individually towards the aggregation centre. As aggregation progresses, cells form head-to-tail contacts with each other, resulting in a string of cells aligned to the aggregation centre. As a result of the good chemotaxis response of wild-type and *gc*-null cells to the spiral waves, the total displacement of the cells before the incorporation into cell streams is about 150-200 μm for each strain. The average radius of the aggregation territories is ~2000 μm for *gc*-null cells and ~2500 μm for wild-type cells. Thus, most of the distance moved towards the aggregation centre is covered while cells are in cell streams, and the formation of stable streams is crucial for efficient aggregation.

Cells that are *gc*-null have a hyperactive rear in contrast to that of wild-type cells, which have a very quiescent rear in streams. If such a lateral protrusion becomes dominant, the cell breaks out of the stream. Thus, even though *gc*-null cells are effective stream formers, make good EDTA-resistant contact sites and exhibit good chemotaxis during the rising flank of the cAMP wave, the persistent loss of directionality between waves increases the rate of stream break-up. This causes many small aggregates to be formed surrounding the initial aggregation centre, culminating in the formation of only small fruiting bodies.

Materials and Methods

Strains and culture conditions

Cells from the AX3 strain were used as a wild type. *gc*-null cells have both guanylyl cyclases *gca* and *sgc* knocked out using homologous recombination in the AX3 strain (Veltman and Van Haastert, 2006). *gbpC*-null cells were created by disrupting the *gbpC* gene in AX3 cells by homologous recombination (L. Bosgraaf and P.v.H., unpublished). Overexpression constructs of full-length sGC, N-terminally truncated sGCΔN and catalytically inactive sGCΔcat are described elsewhere (Veltman and Van Haastert, 2006). All cell strains were grown on Petri dishes under HG5 medium (containing per litre: 14.3 g oxoid pepton, 7.15 g bacto

yeast extract, 1.36 g $Na_2HPO_4 \times 12H_2O$, 0.49 g KH_2PO_4, 10.0 g glucose). When grown with selection, HG5 medium was supplemented with 10 μg/ml G418 or 50 μg/ml hygromycin.

Cell assays

Vegetative cells were harvested, washed twice in 17 mM phosphate buffer, pH 6.5 and settled on non-nutrient agarose (1.5% agarose in 17 mM phosphate buffer). Superfluous buffer was aspirated and humidity was kept at 100% to prevent cells from drying out. Different cell densities were used according to the observation needs. To observe development of a cell strain (Fig. 1), a confluent cell monolayer was used. This corresponded to a cell density of ~1×10^6 cells/cm^2. To monitor chemotaxis of individual cells (Fig. 2), the cell density was reduced to 2.5×10^5 cells/cm^2. Analysis of pseudopod extension was examined at a low cell density (<5×10^4 cells/cm^2) in the steady-state gradient generated by a modified Zigmond chamber (Veltman and Van Haastert, 2006).

Chemotaxis of aggregating cells was analyzed using a combination of VirtualDub (www.virtualdub.org), ImageJ (rsb.info.nih.gov/ij) and Excel (Microsoft Corporation, Redmond, WA). The position of the centroid of each cell in the movie was determined every 30 seconds, yielding a series of coordinates for each cell. Using these coordinates, the velocity and chemotaxis index (the ratio of cell displacement in the direction of the gradient and the total distance travelled) of every step was calculated, yielding a series of velocities and chemotaxis indices for each cell in the movie.

For Fig. 2D, the time points of the maximum chemotaxis index were noted for all waves in the transition period. This corresponded to the responses to cAMP waves 5 to 9 in Fig. 2C for both AX3 and *gc*-null cells. The values of the chemotaxis indices at these time points were averaged (this is time point 0 in Fig. 2D). The values of the preceding and following 15 time points were also averaged, resulting in a series of average chemotaxis indices, spanning a total of two wave periods.

The position of AX3 and *gc*-null cells in streams was monitored as follows. GFP was expressed in wild-type AX3 and in *gc*-null cells. AX3, *gc*-null, AX3(GFP) and *gc*-null (GFP) cells were starved overnight at 4°C. Under these conditions, cells become highly elongated but do not enter the streaming stage. Labelled cells from one strain were mixed 50:50 with unlabeled cells from the other strain, and vice versa. Mixed cell suspensions were settled on non-nutrient agarose at a density of 5×10^4 cells/cm^2 at 22°C and allowed to start streaming. After 1 hour, all cells in streams were identified and the position of fluorescent cells in the stream was noted. The experiment was repeated twice.

For the measurement of the duration of cell-cell contact, AX3 cells and *gc*-null cells were starved overnight at 4°C and settled on non-nutrient agarose at a density of 5×10^4 cells/cm^2. Cells were recorded throughout aggregation and the resulting movie was analyzed as follows: for all cells that made head-to-tail cell-cell contact with another cell, the duration of this contact was noted. Only cells that made contact for >30 seconds were taken into account in order to exclude coincidental contacts. At least four movies were analysed for each cell strain.

Cell adhesion was measured as follows: cells were starved in shaken suspension at a density of 1×10^7 cells/ml. Each hour, a 1 ml sample was drawn and incubated for 15 minutes in 10 mM EDTA. Samples were tumbled slowly during this period to keep the cells in suspension. The number of cells that made no cell contact with other cells was counted using a haemocytometer. The percentage of loose cells was calculated as the ratio of counted single cells per sample to the total number of counted cells at t=0. The percentage of clumped cells was calculated as the total number of cells minus the percentage of loose cells. Each time-point was taken in duplicate, and the experiment was repeated twice.

References

Alcantara, F. and Monk, M. (1974). Signal propagation during aggregation in the slime mould Dictyostelium discoideum. *J. Gen. Microbiol.* **85**, 321-334.

Andrew, N. and Insall, R. H. (2007). Chemotaxis in shallow gradients is mediated independently of PtdIns 3-kinase by biased choices between random protrusions. *Nat. Cell Biol.* **9**, 193-200.

Beug, H., Katz, F. E. and Gerisch, G. (1973). Dynamics of antigenic membrane sites relating to cell aggregation in Dictyostelium discoideum. *J. Cell Biol.* **56**, 647-658.

Bosgraaf, L. and van Haastert, P. J. (2006). The regulation of myosin II in Dictyostelium. *Eur. J. Cell Biol.* **85**, 969-979.

Bosgraaf, L., Russcher, H., Smith, J. L., Wessels, D., Soll, D. R. and Van Haastert, P. J. M. (2002). A novel cGMP signalling pathway mediating myosin phosphorylation and chemotaxis in Dictyostelium. *EMBO J.* **21**, 4560-4570.

Chandrasekhar, A., Wessels, D. and Soll, D. R. (1995). A mutation that depresses cGMP phosphodiesterase activity in Dictyostelium affects cell motility through an altered chemotactic signal. *Dev. Biol.* **169**, 109-122.

Clow, P. A. and McNally, J. G. (1999). In vivo observations of myosin II dynamics support a role in rear retraction. *Mol. Biol. Cell* **10**, 1309-1323.

de la Roche, M. A., Smith, J. L., Betapudi, V., Egelhoff, T. T. and Cote, G. P. (2002). Signaling pathways regulating Dictyostelium myosin II. *J. Muscle Res. Cell Motil.* **23**, 703-718.

Heid, P. J., Wessels, D., Daniels, K. J., Gibson, P., Zhang, H., Voss, E. and Soll, D. R. (2004). The role of myosin heavy chain phosphorylation in Dictyostelium motility, chemotaxis and F-actin localization. *J. Cell Sci.* **117**, 4819-4835.

Kriebel, P. W., Barr, V. A. and Parent, C. A. (2003). Adenylyl cyclase localization regulates streaming during chemotaxis. *Cell* **112**, 549-560.

Merlot, S. and Firtel, R. A. (2003). Leading the way: Directional sensing through phosphatidylinositol 3-kinase and other signaling pathways. *J. Cell Sci.* **116**, 3471-3478.

Muller, K., Gerisch, G., Fromme, I., Mayer, H. and Tsugita, A. (1979). A membrane glycoprotein of aggregating Dictyostelium cells with the properties of contact sites. *Eur. J. Biochem.* **99**, 419-426.

Roelofs, J. and Van Haastert, P. J. M. (2002). Characterization of two unusual guanylyl cyclases from *Dictyostelium*. *J. Biol. Chem.* **277**, 9167-9174.

Roelofs, J., Meima, M., Schaap, P. and Van Haastert, P. J. M. (2001a). The Dictyostelium homologue of mammalian soluble adenylyl cyclase encodes a guanylyl cyclase. *EMBO J.* **20**, 4341-4348.

Roelofs, J., Snippe, H., Kleineidam, R. G. and Van Haastert, P. J. M. (2001b). Guanylate cyclase in *Dictyostelium discoideum* with the topology of mammalian adenylate cyclase. *Biochem. J.* **354**, 697-706.

Ross, F. M. and Newell, P. C. (1979). Genetics of aggregation pattern mutations in the cellular slime mould Dictyostelium discoideum. *J. Gen. Microbiol.* **115**, 289-300.

Ross, F. M. and Newell, P. C. (1981). Streamers: chemotactic mutants of Dictyostelium discoideum with altered cyclic GMP metabolism. *J. Gen. Microbiol.* **127**, 339-350.

Soll, D. R., Wessels, D., Heid, P. J. and Zhang, H. (2002). A contextual framework for characterizing motility and chemotaxis mutants in Dictyostelium discoideum. *J. Muscle Res. Cell Motil.* **23**, 659-672.

Swanson, J. A. and Taylor, D. L. (1982). Local and spatially coordinated movements in Dictyostelium discoideum amoebae during chemotaxis. *Cell* **28**, 225-232.

Van Haastert, P. J. and Devreotes, P. N. (2004). Chemotaxis: signalling the way forward. *Nat. Rev. Mol. Cell Biol.* **5**, 626-634.

van Haastert, P. J. M., van Lookeren Campagne, M. M. and Ross, F. M. (1982). Altered cGMP phosphodiesterase activity in chemotactic mutants of Dictyostelium discoideum. *FEBS Lett.* **147**, 149-152.

Varnum, B., Edwards, K. B. and Soll, D. R. (1985). Dictyostelium amebae alter motility differently in response to increasing versus decreasing temporal gradients of cAMP. *J. Cell Biol.* **101**, 1-5.

Varnum-Finney, B., Edwards, K. B., Voss, E. and Soll, D. R. (1987). Amebae of *Dictyostelium discoideum* respond to an increasing temporal gradient of the chemoattractant cAMP with a reduced frequency of turning: evidence for a temporal mechanism in ameboid chemotaxis. *Cell Motil. Cytoskeleton* **8**, 7-17.

Veltman, D. M. and Van Haastert, P. J. (2006). Guanylyl cyclase protein and cGMP product independently control front and back of chemotaxing Dictyostelium cells. *Mol. Biol. Cell* **17**, 3921-3929.

Wessels, D., Schroeder, N. A., Voss, E., Hall, A. L., Condeelis, J. and Soll, D. R. (1989). cAMP-mediated inhibition of intracellular particle movement and actin reorganization in Dictyostelium. *J. Cell Biol.* **109**, 2841-2851.

Wessels, D. J., Zhang, H., Reynolds, J., Daniels, K., Heid, P., Lu, S., Kuspa, A., Shaulsky, G., Loomis, W. F. and Soll, D. R. (2000). The internal phosphodiesterase RegA is essential for the suppression of lateral pseudopods during Dictyostelium chemotaxis. *Mol. Biol. Cell* **11**, 2803-2820.

Zhang, H., Wessels, D., Fey, P., Daniels, K., Chisholm, R. L. and Soll, D. R. (2002). Phosphorylation of the myosin regulatory light chain plays a role in motility and polarity during Dictyostelium chemotaxis. *J. Cell Sci.* **115**, 1733-1747.